Large Bandwidth Phase-Sensitive DAS with Novel Polarization-Multiplexed Probing Technique

Elie Awwad, Christian Dorize, Patrick Brindel, Ugo Bertuzzi,
Jérémie Renaudier and Gabriel Charlet

Nokia Bell Labs Paris-Saclay, 1 route de Villejust, 91620 Nozay, FRANCE

{elie.awwad, christian.dorize}@nokia-bell-labs.com

Abstract: We propose new polarization-coded binary sequences based on complementary codes to enhance the performance of FBG-based sensor arrays. Speech signals are sensed from the optical phase with linear magnitude and frequency responses up to 18 kHz.

1. Introduction

Distributed acoustic sensing (DAS) is of great interest in monitoring applications such as structural health, railway and pipeline surveillance. Sensitivity, spatial resolution, maximum reach and covered bandwidth are key features of a sensor. Most Rayleigh-based coherent ϕ-OTDR systems are based on interrogations with single or multiple light impulses or frequency sweeps [1,2]. A main limitation of these systems is a tradeoff between the spatial resolution and the maximum reach given that a high spatial resolution forces the use of short pulses resulting in a low signal-to-noise ratio (SNR). Moreover, they are vulnerable to polarization fading effects, unless a dual-polarization coherent receiver is used as in [3,4], given that the Rayleigh backscattered light is polarization dependent. In order to enhance the SNR (thus the sensitivity) of coherent ϕ-OTDR systems, our approach consists in continuously probing the sensor using a training sequence that modulates two orthogonal polarization states of the optical carrier injected in the fiber as done in [3]. While random binary sequences are used to probe a 500 m-long sensor and detect a sinusoidal strain of 500 Hz in [3], we introduce optimized probing sequences of finite length [5] that allow to extend the covered bandwidth. The proposed DAS scheme consists in transmitting polarization-multiplexed coded sequences designed from complementary Golay pairs, and detecting the backscattered optical signal using a polarization-diversity coherent receiver typically used in optical fiber transmission systems followed by a correlation-based post-processing to extract the channel response. As Rayleigh backscattering is randomly distributed along the fiber and the distributed scatterers reflect different amounts of energy, in order to concentrate on the performance of the new scheme, the experimental part of this paper focuses on a fiber sensor with inserted FBGs that turn the fiber into a sensor array, as in [6], with a resolution of 10 m. We show that the proposed DAS solution is capable of spatially resolving speech signals (up to 18 kHz dynamic strains) with a fairly linear magnitude response.

2. Polarization-diversity Coded Sequences

During a period of N symbol times, we modulate the x (resp. y) polarization of the optical signal at the transmitter side by N-long sequences $E_{tx}(n) = G_{xI}(n) + iG_{xQ}(n)$ (resp. $E_{ty}(n) = G_{yI}(n) + iG_{yQ}(n)$) at a symbol-rate $F_S = 1/T_S$. Let $E_{rx}(n)$ and $E_{ry}(n)$ be the sampled outputs of a coherent polarization diversity receiver given by:

$$E_{rx}(n) = h_{xx}(n) * E_{tx}(n) + h_{xy}(n) * E_{ty}(n) \quad , \quad E_{ry}(n) = h_{yx}(n) * E_{tx}(n) + h_{yy}(n) * E_{ty}(n) \tag{1}$$

where $h_{xx}(n), h_{xy}(n), h_{yx}(n), h_{yy}(n)$ are the impulse responses of the channel. At the receiver side, a correlation is performed between the received signals $E_{rx}(n)$ and the sent codes $E_{tx}(n)$ to extract $h'_{xx,xy,yx,yy}(n)$ the estimates of the channel. In order to perform a perfect channel estimation, strict orthogonality conditions should be met as shown in [5] where we chose two mutually orthogonal pairs of complementary (Golay) codes [7] $\{G_{a1}, G_{b1}\}$ and $\{G_{a2}, G_{b2}\}$ to design binary coded sequences meeting these conditions. $\{G_{a1}, G_{b1}\}$ and $\{G_{a2}, G_{b2}\}$ satisfy:

$$
\begin{aligned}
G_{a1}(n) \otimes G_{a1}(n) + G_{b1}(n) \otimes G_{b1}(n) = \delta(n) \quad &\quad G_{a1}(n) \otimes G_{a2}(n) + G_{b1}(n) \otimes G_{b2}(n) = 0 \\
G_{a2}(n) \otimes G_{a2}(n) + G_{b2}(n) \otimes G_{b2}(n) = \delta(n) \quad &\quad G_{a1}(n) \otimes G_{b1}(n) + G_{a2}(n) \otimes G_{b2}(n) = 0
\end{aligned}
\tag{2}
$$

The proof of existence of mutually orthogonal pairs of complementary sequences can be found in [8]. One basic example set of sequences of size $N_G = 4$ satisfying these properties is: $G_{a1}^4 = [1, -1, -1, -1]$, $G_{b1}^4 = [-1, 1, -1, -1]$, $G_{a2}^4 = [-1, -1, 1, -1]$, $G_{b2}^4 = [1, 1, 1, -1]$. Larger sequences of length $N_G = 2^{p+2}, p \geq 1$ are derived recursively [5] . Two polarization-multiplexed mappings using binary or quadrature phase-shift-keying (BPSK or QPSK) modulations on each polarization were covered in [5].The QPSK version considered here consists in simultaneously sending each pair in phase and in quadrature such as $E_{tx}(n) = G_{a1}(n) + iG_{b1}(n)$ and $E_{ty}(n) = G_{a2}(n) + iG_{b2}(n)$ which is unfortunately not enough to guarantee a perfect estimation. However, an additional condition should be met in the specific case of a sensor array in order to fulfil this goal [5]: for a standard equally-spaced-FBG sensor array, the symbol rate must match $F_S = 1/T_S = 4p(\frac{c_f}{2d_s})$ where d_s is the distance between two consecutive FBGs, $p \in \mathbb{N}^*$ and $c_f = c/n_g$, n_g being the group refractive index of the fiber and c the velocity of light.

After the correlation process, we recover the response of each segment between two FBG reflectors and extract the evolution of the optical phase and the polarization state. In this paper, we concentrate on the optical phase ϕ computed as half the phase of the determinant of the dual-pass Jones matrix of each segment at the subsequent FBG reflector: $\phi = 0.5\angle(h'_{xx}h'_{yy} - h'_{xy}h'_{yx})$. The phase is periodically estimated to capture its evolution at each sensor and at consecutive times, achieving a spatio-temporal map of the mechanical/acoustic events surrounding the sensor array with a spatial resolution of d_s and an estimate computed each $T_{code} = NT_S$ seconds. Being interested in the phase evolution in each fiber segment, the differential phase can be computed with the first reflected phase selected as a reference.
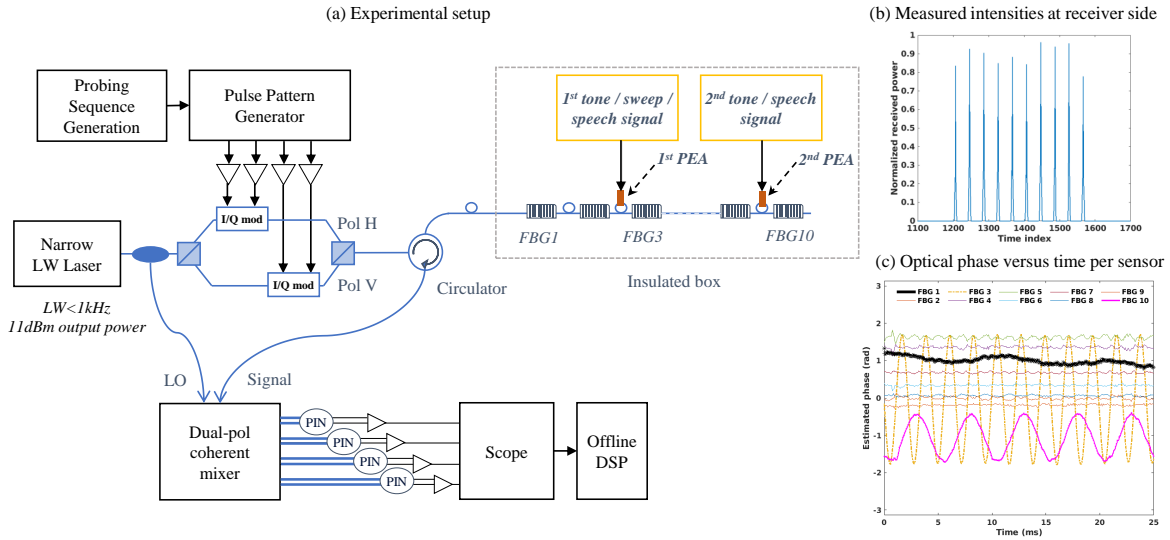
Fig. 1. (a) Experimental Setup: sensor array with ten 10m-spaced FBGs having a reflectivity of -30 dB at 1549.1 nm, PEA: piezo-electric actuator. (b) Measured intensity showing the 10 reflected peaks. (c) Estimated optical phases at the 10 FBG reflectors.

3. Experimental Setup

The experimental setup consists of a dual-polarization I/Q transmitter and a polarization-diversity coherent receiver forming the interrogator connected to the sensor array through an optical circulator as shown in Fig. 1. The light from a RIO^{TM} laser with 600 Hz-linewidth is split into two to be used as a probe at the transmitter and a local oscillator at the receiver. The sensor array consists of 10 FBGs with a reflectivity of 10^{-3} separated by 10 m of fiber. The dual path optical delay between two d_s-spaced FBG reflectors is $\tau_s = 2n_g d_s/c$. The symbol duration T_S has to be selected to fulfil $T_S = \tau_s/K$ where $K \geq 1$ is an integer. For $d_s = 10$ m, the symbol-rate has to be chosen as a multiple of 40 MHz. The probing sequences are continuously generated without any guard band. At the receiver side, the four photocurrents I_X, Q_X, I_Y, Q_Y, detected by balanced photodiodes of 1.6 GHz bandwidth, are sampled at 500 MHz by an oscilloscope during a measurement window T_{acq}. The sensor array is inserted in an insulated box, and is excited at two locations by cylindrical piezoelectric transducers (PZTs) with an outer diameter of 5 cm: one between the second and third FBG (at 25 m from the circulator) and another between the ninth and tenth FBG (at 95 m from the circulator). The PZTs are excited by various electrical signals: first by pure tones and later by 1 s-long speech signals.

4. Experimental Results

The phase stability is first demonstrated when the sensor array, continuously probed at a symbol rate of 160 MSymbol/s, does not endure any mechanical perturbation. For each transmitted code, a synchronization is done based on the intensity response shown in Fig. 1(b), then the phase at each FBG position is extracted from the estimated Jones matrix. The procedure is periodically repeated for each received code over a 20 ms window. To assess phase noise level, we average, over all FBGs and all detected codes, the standard deviation of the estimated phase per FBG. Note that the first FBG serves as an optical phase reference, thus it is excluded from the averaging. Phase standard deviations lower than 20 mrad are measured for a received signal power of -27 dBm and a local oscillator power of 7 dBm. This value is stable for various PDM-QPSK complementary code lengths between 6.4 and 1638.4 μs as shown in Fig. 2(a). Below 6.4 μs, the collected energy per code becomes low compared to the noise level at the receiver, whereas for codes longer than 1638.4 μs, we are limited by phase noise given that the code spreads over a period exceeding the laser coherence time. Between these two limits (correlation noise and coherence loss), the code length can be selected according to the required system bandwidth $BW = 1/(2T_{code})$ as long as $T_{code} > T_{IR}$ where T_{IR} is the duration of the sensor array impulse response.
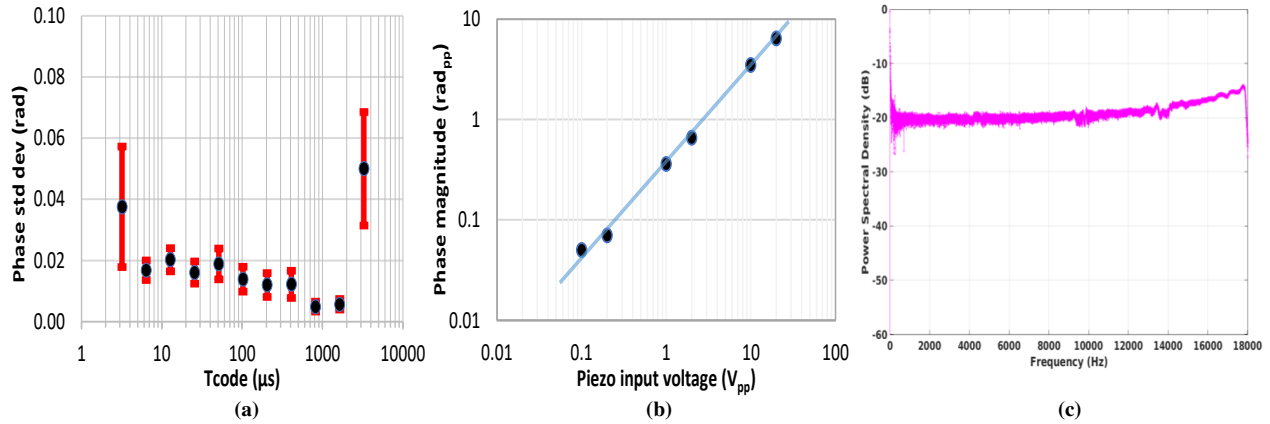
Fig. 2. (a) Standard deviation of estimated phases as a function of T_{code}. (b) Estimation of the dynamic range and (c) power spectral response of the system.

1.5 m of fiber is wrapped around each PZT leading to 25 nm of fiber extension per one volt of excitation voltage, and a 1 rad phase shift measured for a 3 V excitation. Fig. 1(c) shows the optical phase versus time measured at each of the 10 FBGs when simultaneously applying a 500 Hz (resp. 200 Hz) sine wave with a 10 V_{pp} (resp. 4 V_{pp}) magnitude on the first (resp. second) PZT, thus highlighting the distributed sensing feature.

To further demonstrate the ability of the proposed system to finely capture a wide range of mechanical signals, it is necessary to quantify the dynamic range, sensitivity, spectral response as well as crosstalk between sensors. Fig. 2(b) shows the phase magnitude as a function of the excitation voltage for a 1 kHz sine wave at one PZT. We observe a linear behavior for voltages between 0.1 and 20 Vpp (maximum value for our low-frequency generator), leading to a dynamic range beyond 20 dB. A noise floor for voltages below 0.1 V is induced by the laser phase noise. Regarding crosstalk between sensors, a minimal rejection of 30 dB was measured over all the remaining unexcited segments. We also estimated the sensitivity (smallest detectable phase change) for several frequencies of the sine wave excitation. Its value in rad/$\sqrt{Hz}$ was computed in the spectral domain as the ratio between the square root of the noise power and the square root of the maximum bandwidth for $T_{code} = 20.5$ μs. A relatively constant sensitivity around 15 μrad/$\sqrt{Hz}$ was measured over [100 − 18000] Hz. Finally, we measured the power spectral response by applying a 1 s-long chirp excitation that linearly explores the audio bandwidth [20 − 18000] Hz. T_{code} was set to 26 μs to provide a 19 kHz mechanical bandwidth. The power spectral density of the phase response from the stimulated sensor is shown in Fig. 2(c). The disturbances visible at low frequencies are due to the limited measurement window, whereas the rise in the response observed above 10 kHz is produced by the first resonance peak of the PZT located at 20 kHz. This rise can be digitally compensated by spectral inversion to achieve a flat power response. The linear response added to the previously showcased dynamic range and sensitivity demonstrates the ability of the system to reliably capture distributed audio/mechanical signals over a wide spectral range as large as the human hearing system.

To qualitatively validate it, we recorded two 1 s-long speech signals. Their magnitude as a function of time are displayed in Fig. 3(a). In the upper part, a female voice pronouncing "F-X-Days" is transmitted to the first PZT and
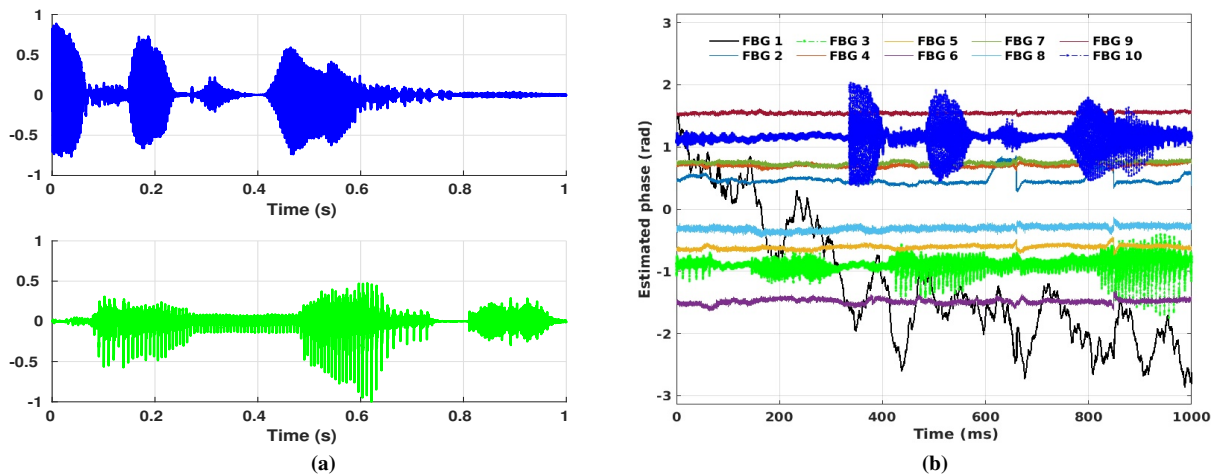
Fig. 3. (a) Time signatures of the two speech signals. (b) Estimated phases captured at the 10 FBGs.

a male voice pronouncing "Bell Labs" is transmitted simultaneously to the second PZT. The choice of speech signals was made because the human voice contains information that spread over a wide bandwidth and within a large dynamic range induced by successions of plosive sounds and stable voiced signals. Fig. 3(b) displays the optical phase versus time measured at each of the 10 FBGs when 26 μs-long PDM-QPSK codes are used. As expected, the two transmitted speech signals are visually recognized, by comparison with Fig. 3(a), at the third and tenth FBGs. We measured, after resampling, synchronization, and normalization, the normalized mean-squared error between the two transmitted signals and the detected phase patterns, and found values lower than 3 %. More interesting is to listen and compare the original and the fairly good quality of the detected signals through the attached .wav audio files [9]. We also added patterns recorded at other unexcited FBGs to highlight the lack of significant crosstalk. Notice that the additive noise, audible in all output phase patterns, is mainly caused by the laser phase noise and may be further reduced when selecting a narrower-linewidth laser source.

5. Conclusion

The performance of newly introduced polarization-coded binary sequences based on complementary Golay codes have been demonstrated. We measured a 20 dB dynamic range over an 18 kHz bandwidth and 30 dB rejection between sensors. We illustrated this performance by listening tests of detected speech signals.

References

1. A. Masoudi and T. P. Newson, "Contributed Review: Distributed optical fibre dynamic strain sensing," Review of Scientific Instruments **87**(1), 011501 (2016).
2. D. Chen, Q. Liu, X. Fan, Z. He, "Distributed fiber-optic acoustic sensor with enhanced response bandwidth and high signal-to-noise ratio," J. Lightw. Techol. **35**(10), 2037-2043 (2017).
3. H.F. Martins, K. Shi, B.C. Thomsen, S. M.-Lopez, M.G.-Herraez, and S.J. Savory, "Real time dynamic strain monitoring of optical links using backreflection of live PSK data," Opt. Express **24**(19), 22303-22318 (2016).
4. Q. Yan, M. Tian, X. Li, Q. Yang, Y. Xu, "Coherent ϕ-OTDR based on polarization-diversity integrated coherent receiver and heterodyne detection," in IEEE 25th Optical Fiber Sensors Conference (OFS), p.1-4 (2017).
5. C. Dorize and E. Awwad, "Enhancing performance of coherent OTDR systems with polarization diversity complementary codes," submitted to Opt. Express, available at http://arxiv.org/abs/1802.06641.
6. F.A.Q. Sun, W. Zhang, T. Liu, Z. Yan, D. Liu, "Wideband fully-distributed vibration sensing by using UWFBG based coherent OTDR," in IEEE/OSA Optical Fiber Communications Conference (OFC), pp. 1-3 (2017).
7. M. Golay, "Complementary series," in IRE Transactions on Information Theory **7**(2), pp. 82-87 (1961).
8. X. Huang, "Complementary Properties of Hadamard Matrices," 2006 International Conference on Communications, Circuits and Systems, pp. 588-592 (2006).
9. Audio files available at https://doi.org/10.6084/m9.figshare.5901478.v1